Journal of Alloys and Compounds 503 (2010) L31–L33

Contents lists available at ScienceDirect

Journal of Alloys and Compounds

journal homepage: www.elsevier.com/locate/jallcom

Letter

Synthesis of iron oxide nanocubes via microwave-assisted solvolthermal method

F.Y. Jiang*, Ch.M. Wang, Y. Fu, R.C. Liu

School of Environment and Materials Engineering, Yantai University, Qingquan Road, Laishan Zone, Yantai, PR China

ARTICLE INFO

Article history:
Received 7 December 2009
Received in revised form 4 May 2010
Accepted 4 May 2010
Available online 11 May 2010

Keywords:
Magnetic materials
Nanomaterials
Solvolthermal
Ostwald ripening

ABSTRACT

Iron oxide nanocubes were prepared by thermal decomposition of iron oleate complex in the presence of oleic acid via microwave-assisted solvolthermal method, followed by Ostwald ripening procedures. X-ray powder diffraction and transmission electron microscopy were used to characterize the structure and morphology of the products. The results revealed that the primary nanoparticles synthesized by microwave heating were low crystalline spheres with an average diameter of about 6 nm. After aging at 180 °C, these iron oxides transform to crystalline α-Fe_2O_3 and trace amount of Fe_3O_4. The influence of aging time on the size and morphology of α-Fe_2O_3 nanocrystals was studied. Room temperature magnetization curves measured to study the magnetic properties of as-synthesized nanoparticles.

1. Introduction

In recent years, magnetic nanoparticles have attracted considerable attention not only for fundamental research, but also for broad range of applications, such as magnetic fluids [1], catalysis [2,3], biotechnology and biomedicine [4], magnetic resonance imaging [5–7], etc. Among these magnetic materials, iron oxides (Fe_2O_3 and Fe_3O_4) have been extensively investigated due to its excellent performance. The synthesis of uniform iron oxide nanoparticles is important because the properties of these nanoparticles depend strongly on their dimensions [7].

Various chemical routes to synthesize iron oxide nanoparticles have been developed, such as coprecipitation [8,9], hydrolysis of iron salt [10,11], decomposition of organic iron precursor [12–15], microemulsion [16], hydrothermal and solvolthermal methods [17–19]. However, the relatively poor size uniformity and low crystallinity of obtained nanoparticles strongly deteriorate their performance. Hence, the synthesis of monodisperse iron oxide nanoparticles with uniform size and high crystallinity remains a challenge.

Microwave can homogeneously heat the reaction medium rapidly, resulting in a blooming of nucleation, which is favorable for small particle size and narrow particle size distribution. The use of microwave in conventional hydrothermal system developed a new technique named microwave-hydrothermal method [20]. Yu et al. reported the synthesis of monodisperse α-Fe_2O_3 nanocrystals with continuous aspect-ratio tuning and fine shape control by such a method [21].

Herein, we report a simple solvolthermal method to prepare uniform α-Fe_2O_3 nanocubes with high crystallinity. In our experiments, a mild microwave-assisted solvolthermal method is used, and an economic and environmentally friendly reagent, $FeCl_3$ serves as Fe source.

2. Experimental

The $Fe(oleate)_3$ complex was synthesized by the reaction between ferric chloride and sodium oleate. In a typical synthesis, 19.00 g of sodium oleate was mixed with 6.38 g of oleic acid, 10 mL of ethanol and 10 mL of water. Subsequently, 28.00 g triethylene glycol was added to above mixture under vigorous stirring to form a homogeneous solution. Then a mixture solution composed of 2.00 g anhydrous ferric chloride ($FeCl_3$, 98%), 10 mL of ethanol and 10 mL of water was added to the above solution dropwise. The mixture was heated to 80 °C and maintained at this temperature for 6 h under continuous stirring. Two phases occurred in the reaction system. The upper layer was henna organic layer containing $Fe(oleate)_3$ complex and oleic acid, whereas the bottom layer was aqueous solution.

The decomposition of $Fe(oleate)_3$ was conducted by a microwave digestion system. The obtained mixture solution was transferred into a Teflon-lined digestion vessel, and subjected to microwave treatment operating at 2.45 GHz with a power of 400 W for 6 min, then cooled down to room temperature naturally. Fine iron oxide nanoparticles can be collected by centrifugation and washed with ethanol three times.

The Ostwald ripening procedure was carried out by transferring the microwave-treated mixture into a Teflon-lined stainless autoclave, and aging in an oven at 180 °C for 10 h and 20 h respectively. When it was cooled to room temperature, the precipitate was collected by centrifugation and washed with ethanol three times.

X-ray diffraction (XRD) patterns were collected on an X'Pert Pro X-ray diffraction meter with Cu Kα radiation (λ = 0.154 nm) operating at 40 kV and 30 mA. The scan range (2θ) was from 10° to 60° with a step of 0.08° and scan speed of 5.00°/min.

* Corresponding author. Tel.: +86 535 6706038; fax: +86 535 6706038.
E-mail address: fyjiang@ytu.edu.cn (F.Y. Jiang).

0925-8388/$ – see front matter © 2010 Elsevier B.V. All rights reserved.
doi:10.1016/j.jallcom.2010.05.020

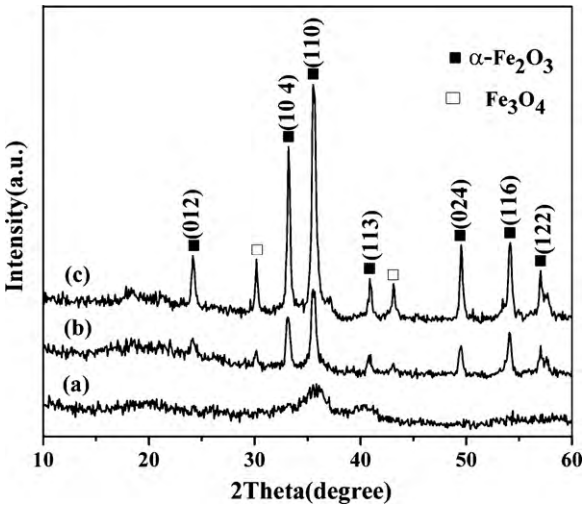

Fig. 1. XRD patterns of iron oxide nanoparticles synthesized via microwave heating (a), and microwave heating followed by aging at 180 °C for 10 h (b) and 20 h (c) respectively.

Transmission electron microscopy (TEM) observation was carried out on JEOL-100CX operating at 100 kV. The samples for TEM observation were prepared by dropping one or two droplets of cyclohexane dispersion of as-synthesized nanoparticles on the carbon-coated copper grids and drying at room temperature. The magnetization curves of as-synthesized nanoparticles were acquired on a LakeShore vibrating sample magnetometer (VSM, model 7037/9509-P) at room temperature.

3. Results and discussion

Fig. 1a shows the XRD pattern of as-synthesized products by microwave heating. No clear peaks can be identified except weak peaks located at 2θ values of 36° and 41°, due to its low crystallinity in the fast nucleation process. The broadening of peak widths indicates the smaller size of the particles.

After aging at 180 °C, diffraction peaks in Fig. 1b and c show the evolution of α-Fe_2O_3 with characteristic peaks of (0 1 2), (1 0 4), (1 1 0), (1 1 3), (0 2 4), (1 1 6) and (1 2 2) (JCPDS 86-0550), which also coincide with the appearance of cubic shaped nanoparticles shown in TEM images. Impure peaks located at 2θ values of 31°, 43° can be assigned to magnetite (Fe_3O_4). Usually, the thermal decomposition of metal carboxylates result in the formation of metal oxide along with other byproducts such as CO, CO_2, H_2, ketones, esters, and hydrocarbons with various chain lengths. Consequently, it seems that a trace amount of CO, H_2, and carbon produced by the thermal decomposition of iron oleate complex is responsible for the reduction of Fe^{3+} to Fe^{2+}, that lead to the appearance of Fe_3O_4. The ratio of integral intensity of Fe_3O_4 diffraction peaks to that of α-Fe_2O_3 for aging 10 h and 20 h are about 0.078 and 0.082, respectively, which indicates that α-Fe_2O_3 is the major product. The peak position and relative intensity of the two ripened samples match well to each other, suggesting that they have the same crystal structure. With an aging time of 20 h, the intensity of peaks increased significantly compared to that of 10 h, indicating the increase of crystallinity and grain size of the nanoparticles.

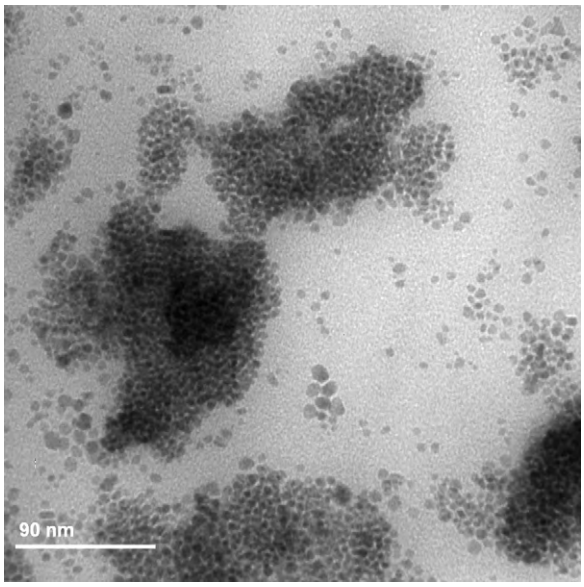

Fig. 2. TEM image of iron oxide nanoparticles synthesized via microwave heating (scale bar: 90 nm).

Fig. 2 shows the TEM image of particles synthesized via microwave heating. During microwave irradiation processes, the rapid nucleation produced relatively uniform small spherical iron oxide nanoparticles with average diameter of about 6 nm. These small nanoparticles have low crystallinity as indicated by XRD results (Fig. 1a).

After aging at 180 °C for 10 h, it has been observed that most particles were cubic with the size of 13 nm and larded with small spherical particles (Fig. 3a). During the aging progress, the small spherical particles change their morphologies gradually through Oswald ripening, in which smaller nanoparticles dissolved and

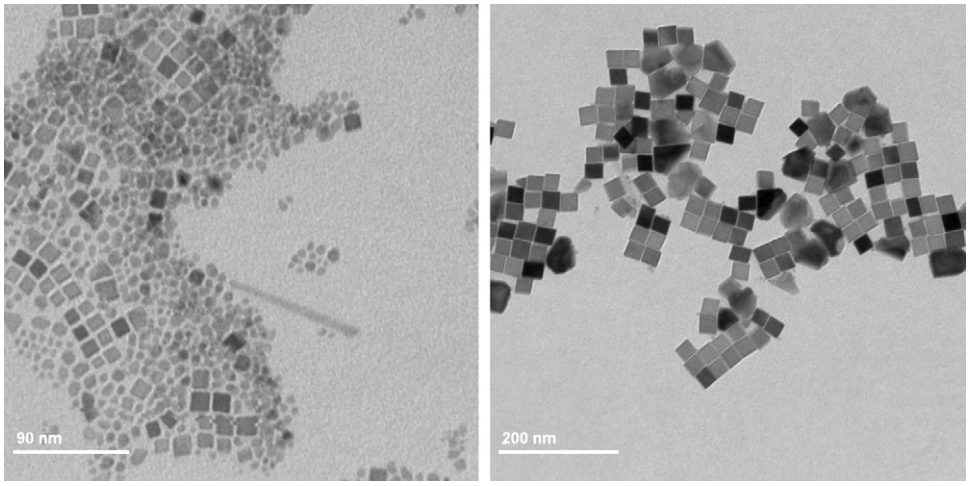

Fig. 3. TEM images of iron oxide nanoparticles synthesized via microwave heating followed by aging at 180 °C for (a) 10 h (scale bar: 90 nm) and (b) 20 h (scale bar: 200 nm).

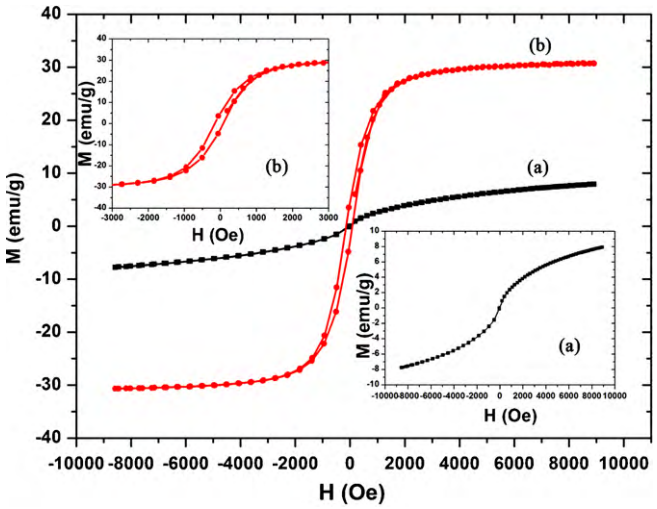

Fig. 4. Room temperature magnetization curves of iron oxide nanoparticles synthesized via microwave heating (a) and microwave heating followed by aging at 180 °C for 20 h (b). Insets are closer look of traces (a) and (b).

redeposited on the surface of bigger nanoparticles. The appearance of cubic nanoparticles coincide with the evolution of α-Fe_2O_3 characteristic peaks in XRD pattern (Fig. 1b and c).

When the aging time was prolonged to 20 h, small particles almost disappeared and the size of cubic particles increased to 28 nm with high crystalline nature (Fig. 3b). But a small amount of large and irregular shaped particles also appeared. So a proper aging time is necessary to obtain uniform nanocubes.

The magnetization curves of as-synthesized iron oxide nanoparticles measured at room temperature are shown in Fig. 4. The saturation magnetization increases from 8 emu/g to 30 emu/g when aging at 180 °C for 20 h. This can be attributed to the growth of particles size and the improvement of crystallinity. Since the hematite (α-Fe_2O_3) is weakly magnetic at room temperature, the relative higher saturation magnetization can be attributed to the presence of Fe_3O_4, which was confirmed by XRD results (Fig. 1). Due to the small particle size, the iron oxide nanoparticles synthesized by microwave heating (Fig. 4(a)) is superparamagnetic at room temperature, but when aging at 180 °C for 20 h, the iron oxide nanoparticles become ferromagnetic that exhibit an obvious hysteresis phenomenon. This is because the particle size already exceeds the critical size of superparamagnetic.

4. Conclusions

Cubic iron oxide nanoparticles were prepared via microwave-assisted solvolthermal method followed by Ostwald ripening procedures. Microwave-solvolthermal produced primary small spherical particles with low crystallinity due to a fast nucleation process. These small particles exhibit superparamagnetic character at room temperature. At the early stage of aging process, cubic shaped crystalline α-Fe_2O_3 with a trace amount of Fe_3O_4 formed, larded with small spherical particles. With the prolonging of aging time, small spherical particles transformed into cubic particles mostly, and a small amount of large and irregular shaped particles appeared, the corresponding magnetic properties change from superparamagnetic to ferromagnetic.

Acknowledgements

This work was supported by National Natural Science Foundation of China (50972123) and Natural Science Foundation of Shandong Province, China (Y2007F19).

References

[1] S. Chikazumi, S. Taketomi, M. Ukita, M. Mizukami, H. Miyajima, M. Setogawa, Y. Kurihara, J. Magn. Magn. Mater. 65 (1987) 245–251.
[2] A.-H. Lu, W. Schmidt, N. Matoussevitch, H. BPnnermann, B. Spliethoff, B. Tesche, E. Bill, W. Kiefer, F. SchVth, Angew. Chem. Int. Ed. 43 (2004) 4303–4306.
[3] S.C. Tsang, V. Caps, I. Paraskevas, D. Chadwick, D. Thompsett, Angew. Chem. Int. Ed. 43 (2004) 5645–5649.
[4] A.K. Gupta, M. Gupta, Biomaterials 26 (2005) 3995–4021.
[5] S. Mornet, S. Vasseur, F. Grasset, P. Verveka, G. Goglio, A. Demourgues, J. Portier, E. Pollert, E. Duguet, Prog. Solid State Chem. 34 (2006) 237–247.
[6] Z. Li, L. Wei, M.Y. Gao, H. Lei, Adv. Mater. 17 (2005) 1001–1005.
[7] Y.W. Jun, Y.M. Huh, J.S. Choi, J.H. Lee, H.T. Song, S. Kim, S. Yoon, K.S. Kim, J.S. Shin, J.S. Suh, J. Cheon, J. Am. Chem. Soc. 127 (2005) 5732–5733.
[8] D.K. Kim, M. Mikhaylova, Y. Zhang, M. Muhammed, Chem. Mater. 15 (2003) 1617–1627.
[9] R. Valenzuela, M.C. Fuentes, C. Parra, J. Baeza, N. Duran, S.K. Sharma, M. Knobel, J. Freer, J. Alloys Compd. 488 (2009) 227–231.
[10] Zh.F. Pu1, M.H. Cao, J. Yang, K.L. Huang, Ch.W. Hu, Nanotechnology 17 (2006) 799–804.
[11] T. Ozkaya, M.S. Toprak, A. Baykal, H. Kavas, Y. Köseoğlu, B. Akta, J. Alloys Compd. 472 (2009) 18–23.
[12] J. Rockenberger, E.C. Scher, A.P. Alivisatos, J. Am. Chem. Soc. 121 (1999) 11595–11596.
[13] H.T. Song, J.S. Choi, Y.M. Huh, S. Kim, Y.W. Jun, J.S. Suh, J. Cheon, J. Am. Chem. Soc. 127 (2005) 9992–9993.
[14] J. Kim, J.E. Lee, J. Lee, Y. Jang, S.W. Kim, K. An, H.H. Yu, T. Hyeon, Angew. Chem. Int. Ed. 45 (2006) 4789–4793.
[15] R. Shi, X.H. Liu, G.H. Gao, R. Yi, G.Zh. Qiu, J. Alloys Compd. 485 (2009) 548–553.
[16] T. Nakanishi, H. Iida, T. Osaka, Chem. Lett. 32 (2003) 1166–1168.
[17] B.P. Jia, L. Gao, Cryst. Growth Design 8 (2008) 1372–1376.
[18] Sh.B. Wang, Y.L. Min, S.H. Yu, J. Phys. Chem. C 111 (2007) 3551–3554.
[19] J. Chen, F.B. Wang, K.L. Huang, Y.N. Liu, S.Q. Liu, J. Alloys Compd. 475 (2009) 898–902.
[20] G.J. Wilson, A.S. Matijasevich, D.R.G. Mitchell, J.C. Schulz, G.D. Will, Langmuir 22 (2006) 2016–2027.
[21] X.L. Hu, J.C. Yu, Adv. Funct. Mater. 18 (2008) 880–887.